

pH-Triggered Echogenicity and Contents Release from Liposomes

Rahul Nahire,[†] Rayat Hossain,[†] Rupa Patel,[†] Shirshendu Paul,[‡] Varsha Meghnani,[†] Avinash H. Ambre,[§] Kara N. Gange,^{||} Kalpana S. Katti,[§] Estelle Leclerc,[†] D. K. Srivastava,[⊥] Kausik Sarkar,^{‡,#} and Sanku Mallik^{*,†}

[†]Department of Pharmaceutical Sciences, North Dakota State University, Fargo, North Dakota 58108, United States

[⊥]Department of Chemistry and Biochemistry, North Dakota State University, Fargo, North Dakota 58108, United States

[§]Department of Civil Engineering, North Dakota State University, Fargo, North Dakota 58108, United States

[‡]Department of Mechanical Engineering, University of Delaware, Newark, Delaware 19716, United States

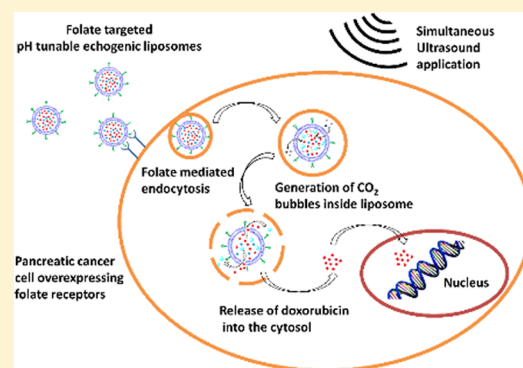
[#]Department of Mechanical and Aerospace Engineering, George Washington University, Washington, D.C. 20052, United States

^{||}Department of Health, Nutrition and Exercise Sciences, North Dakota State University, Fargo, North Dakota 58108, United States

S Supporting Information

ABSTRACT: Liposomes are representative lipid nanoparticles widely used for delivering anticancer drugs, DNA fragments, or siRNA to cancer cells. Upon targeting, various internal and external triggers have been used to increase the rate for contents release from the liposomes. Among the internal triggers, decreased pH within the cellular lysosomes has been successfully used to enhance the rate for releasing contents. However, imparting pH sensitivity to liposomes requires the synthesis of specialized lipids with structures that are substantially modified at a reduced pH. Herein, we report an alternative strategy to render liposomes pH sensitive by encapsulating a precursor which generates gas bubbles *in situ* in response to acidic pH. The disturbance created by the escaping gas bubbles leads to the rapid release of the encapsulated contents from the liposomes. Atomic force microscopic studies indicate that the liposomal structure is destroyed at a reduced pH. The gas bubbles also render the liposomes echogenic, allowing ultrasound imaging. To demonstrate the applicability of this strategy, we have successfully targeted doxorubicin-encapsulated liposomes to the pancreatic ductal carcinoma cells that overexpress the folate receptor on the surface. In response to the decreased pH in the lysosomes, the encapsulated anticancer drug is efficiently released. Contents released from these liposomes are further enhanced by the application of continuous wave ultrasound (1 MHz), resulting in substantially reduced viability for the pancreatic cancer cells (14%).

KEYWORDS: pH-sensitive liposomes, ultrasound, drug delivery, echogenic liposomes, pancreatic cancer



INTRODUCTION

Among the lipid nanoparticles, liposomes are widely studied as drug delivery vehicles.^{1–3} Liposomes protect the encapsulated drugs from being metabolized during the circulation prior to reaching the target. The US Food and Drug Administration has approved liposome-based formulations for the treatment of several types of cancer.⁴ However, upon targeting, the passive release of the encapsulated drugs from the liposomes is often slow.⁵ Reorganization of the lipid domains has been used as a trigger to enhance, and to control the rate and the extent of contents released from liposomes.^{6–8} Among the various triggers, decreased pH in the lysosomes has been widely used as a successful strategy to efficiently release the encapsulated liposomal contents.^{9,10} However, imparting pH sensitivity to liposomes requires the synthesis of specialized lipids with structures that are substantially modified, either due to hydrolysis or due to changes in the protonation states of the lipid head groups, at reduced pH.^{9,11–13}

Stabilized gas bubbles are widely used as contrast-enhancing agents for ultrasound imaging of perfused tissues.¹⁴ There are many reports of ultrasound-mediated drug release from nanoparticles, liposomes, and other carriers.^{15–21} The majority of these studies were conducted employing kHz frequency ultrasound.^{22–24} Although ultrasound waves in the kHz frequency efficiently release drugs from the carriers (due to cavitation and high local temperatures), the harmful biological effects associated with low-frequency ultrasound limit the usefulness of such strategies.²⁵ To make liposomes responsive to high-frequency ultrasound, they need to be coupled with gas pockets. Echogenic liposomes (ELIPs) entrap small amounts of air along with the hydrophilic drug in their aqueous interior,

Received: March 7, 2014

Revised: September 15, 2014

Accepted: October 1, 2014

Published: October 1, 2014

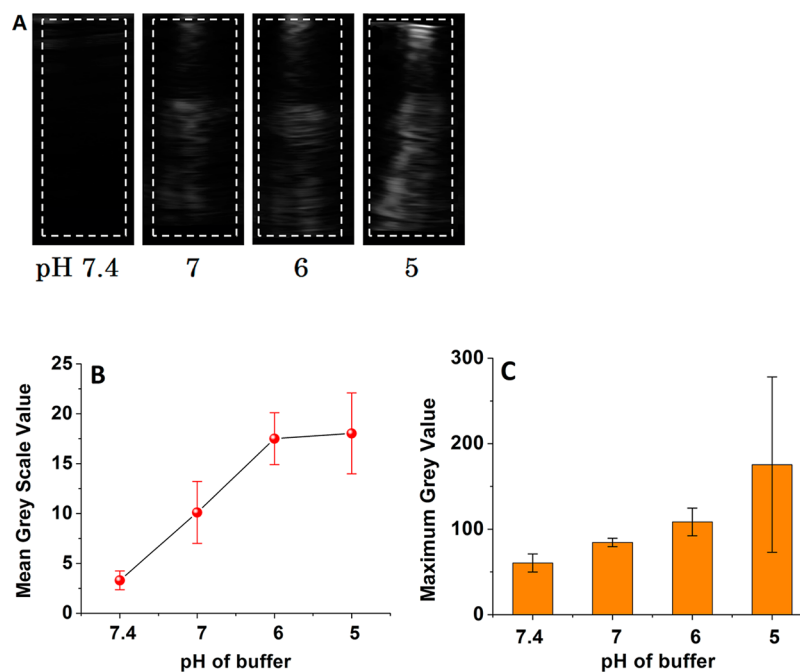


Figure 1. (A) pH-dependent diagnostic frequency ultrasound imaging of POPC liposomes encapsulating 400 mM ammonium bicarbonate. The dotted white lines represent the regions of interest (ROI) that were used to calculate the gray scale values. (B) Mean gray scale values and (C) maximum gray scale values for the ultrasound images shown in panel A as a function of pH ($n = 3$).

and are currently being developed as drug delivery vehicles for ultrasound-triggered drug release and simultaneous imaging.^{26–28} Although there is uncertainty about the exact location and size of the entrapped air bubbles in the ELIPs, their acoustic characterization has been reported extensively in the literature.^{29–32}

We are developing targeted, multimodal liposomes for triggered release of encapsulated contents, and simultaneous ultrasound imaging. Furthermore, we are interested in enhancing the contents released from the liposomes by employing diagnostic frequency (MHz) ultrasound. We have recently demonstrated the ultrasound-enhanced, extracellular release of liposomal contents mediated by the cancer-cell-secreted enzyme matrix metalloproteinase-9 (MMP-9).³³ Herein, we report a strategy to render liposomes pH sensitive by encapsulating ammonium bicarbonate which generates gas bubbles *in situ* in response to acidic pH.³⁴ Our strategy does not require the use of pH-sensitive lipids in the liposomal formulations. We hypothesize that, at a reduced pH, the hydronium ions diffuse into the aqueous interior of the liposomes, and produce carbon dioxide bubbles, thereby “turning on” the echogenicity. We have successfully imaged the liposomes by employing a medical ultrasound scanner. As more bubbles are generated, the liposomal bilayer is disturbed, leading to the release of encapsulated contents. We observe that the release was further enhanced by applying ultrasound with a frequency of 1 MHz. To the best of our knowledge there are no reports in the literature of ultrasound enhanced triggered release from pH-tunable echogenic liposomes.

We have demonstrated the usefulness of this liposomal delivery system using the PANC-1 pancreatic cancer cells. Pancreatic cancer is one of the leading causes of cancer-related deaths in both men and women in the United States, with a 5-year survival rate of less than 5%.^{35,36} According to the American Cancer Society, 38,460 pancreatic cancer related

deaths (almost equally split between men and women) occurred in United States in 2013.

■ EXPERIMENTAL SECTION

All experimental details are provided in the Supporting Information.

■ RESULTS AND DISCUSSION

Preparation of Liposomes Encapsulating Ammonium Bicarbonate and the Demonstration of pH-Tunable Echogenicity. To demonstrate tunable echogenicity, we prepared the liposomes from 1-palmitoyl-2-oleoyl-*sn*-glycero-3-phosphocholine (POPC), encapsulating 400 mM ammonium bicarbonate along with the self-quenching dye carboxyfluorescein (100 mM). We reasoned that, for multilamellar liposomes, the outside hydronium ions need to diffuse through several lipid bilayers in order to generate sufficient amounts of CO₂ gas inside the liposomes. The presence of several lipid bilayers was also expected to decrease the efficiency of the contents released in response to escaping gas bubbles and ultrasonic excitation. Hence, we decided to formulate unilamellar liposomes with a narrow size distribution by sonicating and sequentially extruding (through 800 and 200 nm polycarbonate membrane filters) the initially formed multilamellar vesicles. We observed (with dynamic light scattering) that the average hydrodynamic diameter of the liposomes is 110 ± 15 nm with a polydispersity index of 0.05 (Supporting Information, Figure S1A). These results were corroborated with transmission electron microscopic imaging of the liposomes (Supporting Information, Figure S1B).

To demonstrate the tunable echogenicity, we added the liposomes to buffers with different pHs (7.4–5.0) and recorded the images using a Terason t3200 high-frequency (12–14 MHz) diagnostic ultrasound transducer. We expected that the generated gas bubbles would reflect the ultrasound, and that the

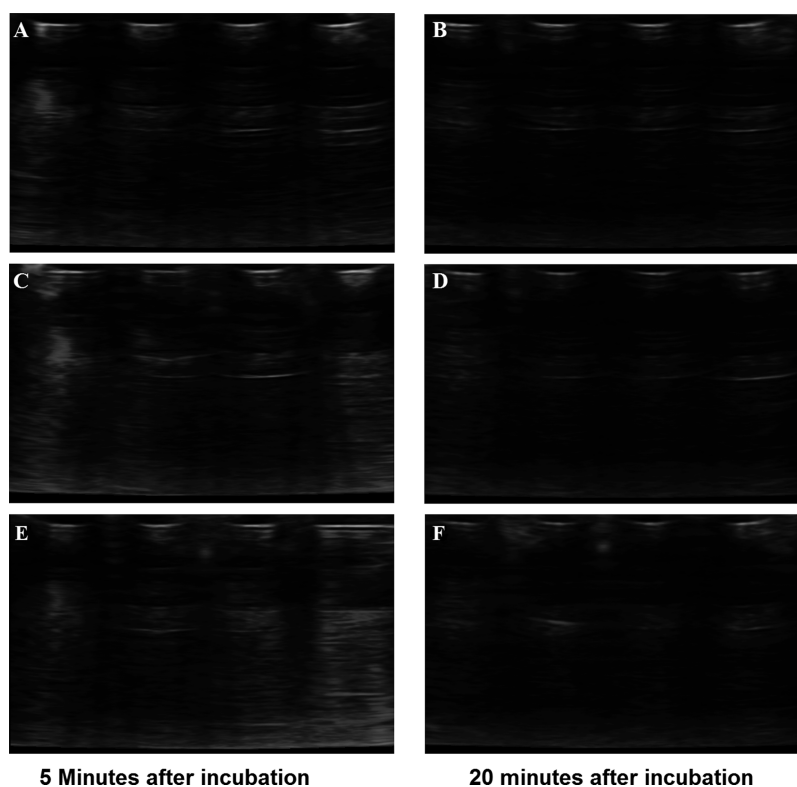


Figure 2. Diagnostic frequency ultrasound images of POPC liposomes encapsulating 400 mM ammonium bicarbonate as a function of frequency and incubation time in a pH 5 buffer. The images were acquired by employing high-frequency (12–15 MHz; A, B), medium-frequency (8–12 MHz; C, D), and low-frequency (4–8 MHz; E, F) ultrasound transducers.

contrast of the images would be more pronounced as the amount of generated gas is increased at a lower pH. We observed that there was a lag time before the liposomes became echogenic, and that the duration of this lag phase decreased with the reduced pH. For example, liposomes in the pH 7.4 buffer did not show any ultrasound contrast in 10 min. At pH 6, the liposomes became weakly echogenic in 5 min, but at pH 5, the liposomes were fairly echogenic within 3 min. The ultrasound images for the liposomes in buffers with different pH values after 5 min are shown in Figure 1. Figure 1A shows that there is no echo at pH 7.4; but as the pH is reduced, progressively stronger echo from the entire cell well is observed (note that the ultrasound probe is placed at the top of the cell well). Figures 1B and 1C show how the mean and maximum gray scale values quantitatively change with pH. The echo from the homogeneous suspension of liposomes appears as light bands (Figure 1A). Such coarse features are common in ultrasound images. They arise due to interference between echoes from subresolution scatterers such as liposomes which themselves are far smaller in size than the ultrasound wavelength.³⁷ The resolution of the figure is 0.1 mm.

We anticipated that the concentration of hydronium ions in the external buffer would affect their diffusion rate inside the liposomes as well as the subsequent generation of CO₂ bubbles. As the encapsulated ammonium bicarbonate was depleted, the generation of CO₂ gas slowed down and finally stopped. Consistent with this hypothesis, we observed that liposomes in the pH 5 buffer are not echogenic after 20 min (Figure 2). However, we noted that the diameters of the gas bubbles inside the liposomes are likely to be small (in nanometers), and that they may not reflect the ultrasound very well.³⁸ It is likely that the nanobubbles coalesce in the lipid bilayer of the liposomes,

generating larger bubbles, and reflect the ultrasound. POPC lipid has a gel low transition temperature (−2 °C), and the liposomal bilayer is in the fluid phase under the experimental conditions (20 °C).³⁹ The loose lipid packing and fluidity of the POPC bilayer accommodate the coalescence and the size increase of the gas bubbles.

We analyzed the ultrasound images shown in Figure 1A using the ImageJ software (<http://rsbweb.nih.gov>) to calculate the mean and maximum gray scale values for region of interest (ROI) shown in Figure 1A. As expected, the mean and maximum gray scale values increase with a decreasing pH. We observed that the highest gray scale value was observed at pH 5, and it does not increase any more below this pH (data not shown). We also observed a time-dependent decrease in the echogenicity of these liposomes at pH 5.0 (Figure 2). These results demonstrated that liposomes are programmed to reflect the ultrasound only after reaching the acidic microenvironment of cancer cells.

pH-Triggered Release of Liposomal Contents and Mechanistic Studies. Having demonstrated pH-tunable echogenicity, we decided to determine if the escaping gas bubbles sufficiently disturb the lipid bilayer to release the encapsulated contents from the liposomes. For this endeavor, we incubated the POPC liposomes (encapsulating carboxyfluorescein and 400 mM ammonium bicarbonate) in buffers with different pH values (7.4–5.0), and monitored the emission intensity of carboxyfluorescein. However, the emission intensity of carboxyfluorescein is quenched as the pH is lowered.⁴⁰ To correct for this decreased emission intensity, we measured the absorption spectra of carboxyfluorescein as a function of pH, and we determined the isosbestic point to be 460 nm. Subsequently, the dye solution was prepared in buffers with pH

of 7.4, 6.0, and 5.0; the solution was excited at 460 nm, and the emission spectra were recorded. We observed that the emission spectra produced an isobestic point at 497 nm. We then monitored the emission of the dye at 497 nm (excitation: 460 nm) for 2 h. The correction factors were calculated at each pH as a function of time, and all emission intensities were appropriately corrected for calculating the percentage released (Supporting Information).

When the liposomes were incubated in acidic buffers, there was a time lag before dye release (Figure 3). However, the

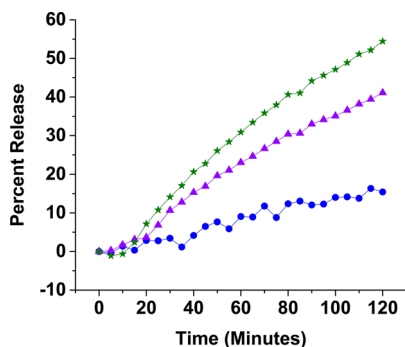


Figure 3. Representative release profiles of carboxyfluorescein from POPC liposomes encapsulating 400 mM ammonium bicarbonate. The liposomes were incubated in buffers with pH 7.4 (blue circles), pH 6.0 (purple triangles), and pH 5.0 (green stars). The lines are generated by connecting the observed data points.

liposomes continued to leak the contents for a considerably long time (2–3 h). The continued leakage indicates that the disturbances in the lipid bilayers created by the escaping gas bubbles either are not sealed or take a long time to heal.

While the liposomes at a pH of 7.4 (control) released only 15% of the encapsulated dye in 2 h, at a pH of 5, the release increased to 55% (Figure 3). When we encapsulated sodium bicarbonate in the liposomes (instead of ammonium bicarbonate), the amount of the content release decreased. In 2 h, we observed that the sodium bicarbonate encapsulated liposomes released 40% of the encapsulated dye (at pH = 5.0; Supporting Information, Figures S3 and S4). For both of these liposomal formulations, the rate of contents release decreased considerably after 2 h. In 3 h at pH 5.0, the ammonium bicarbonate encapsulated liposomes released 75% of the contents, and the sodium bicarbonate encapsulated liposomes released 44% of the contents (Figure 4A). Decreasing the amount of encapsulated ammonium bicarbon-

ate (from 400 mM to 200 mM) also reduced the amount of contents release from the liposomes (Figure 4B).

The acidic decomposition of ammonium bicarbonate generates NH_3 and CO_2 , while sodium bicarbonate produces the sodium salt of the buffer, H_2O , and CO_2 . The ammonia gas will react with the hydronium ions in the liposome interior, leading to a reduction in proton concentration. The resultant proton gradient will facilitate the diffusion of more hydronium ions into the liposomal lumen and generate more CO_2 gas and ammonia. Amount of generated gas decreases by reducing the concentration of encapsulated ammonium bicarbonate (from 400 to 200 mM), leading to a reduction in contents release from the liposomes (Figure 4B). As an additional control, we prepared the POPC liposomes without encapsulating any gas precursor and studied the contents release as a function of pH. We observed minimal release (<10%) of the encapsulated carboxyfluorescein at pH 7.4 and 6.0. However, at pH 5.0, about 20% of the dye was released in 2 h (Figure S5, Supporting Information). We do not have an explanation for this observation yet.

In these liposome formulations, we used POPC as the bilayer forming lipid. The POPC molecules contain the saturated palmitoyl and the unsaturated oleoyl groups. Due to the presence of an alkene in the Z-configuration, this lipid does not form a tight bilayer, and the gel transition temperature is also low (-2°C).³⁹ It is possible that the loose packing of the POPC lipids will likely allow the escaping CO_2 bubbles to coalesce inside the hydrophobic bilayer of the liposomes. The resulting larger gas bubbles will disturb the bilayer while escaping, allowing the contents to leak. To determine if the lipid packing in the liposomal bilayer and the gel transition temperature affect the contents released, we prepared two batches of DSPC (1,2-distearoyl-*sn*-glycero-3-phosphocholine) liposomes that encapsulate ammonium and sodium bicarbonate respectively (400 mM each). The DSPC molecules contain two saturated stearoyl groups and form a tight bilayer with a melting temperature of 56°C .⁴¹ We hypothesized that the tightly packed lipid molecules in the bilayer would hinder the coalescence of the escaping CO_2 bubbles generated inside the aqueous core of the liposomes. This would result in minimal contents release from the DSPC liposomes. In addition, the rate of diffusion of the hydronium ions across the lipid bilayer would be slower compared to the POPC bilayer. We observed that both ammonium bicarbonate and sodium bicarbonate encapsulated DSPC liposomes released less than 5% of their contents after incubation for 2 h at a pH of 5.0 (Supporting Information, Table S1).

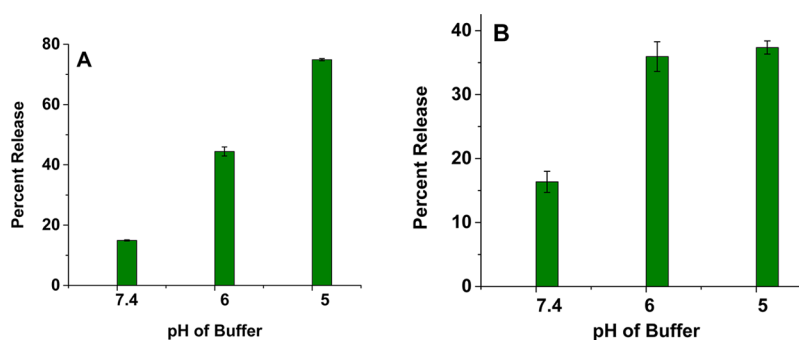


Figure 4. Release of encapsulated carboxyfluorescein from POPC liposomes as a function of pH encapsulating (A) 400 mM ammonium bicarbonate and (B) 200 mM ammonium bicarbonate after 3 h ($n = 3$).

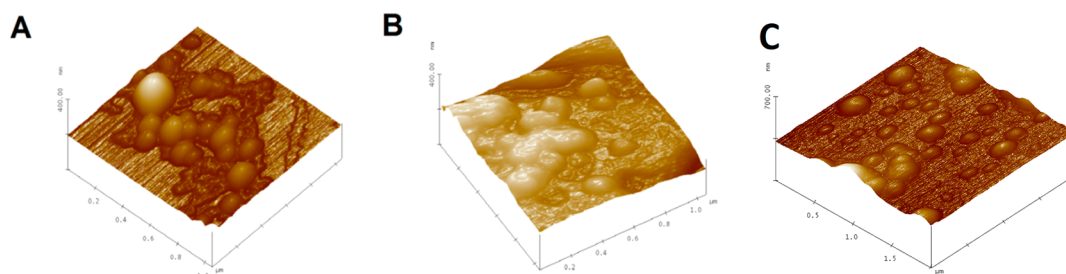


Figure 5. Atomic force microscopic images of pH-tunable echogenic POPC liposomes. (A) Liposomes containing 400 mM ammonium bicarbonate before incubation. (B) Liposomes containing 400 mM ammonium bicarbonate after incubation in pH 5 buffer for an hour. (C) Buffer containing liposomes after incubation in a pH 5 buffer for an hour.

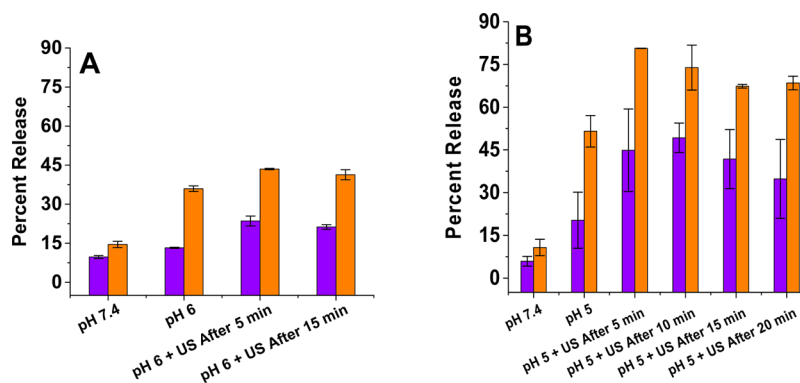


Figure 6. Ultrasound-enhanced (1 MHz, CW, 2 W/cm², 5 min), pH-triggered release from POPC liposomes encapsulating 400 mM ammonium bicarbonate at pH = 6.0 (A) and pH = 5.0 (B). The release values at a pH of 7.4 are included as the controls. Violet bars: release after 20 min with ultrasound application. Orange bars: release after 2 h with ultrasound application ($n = 3$).

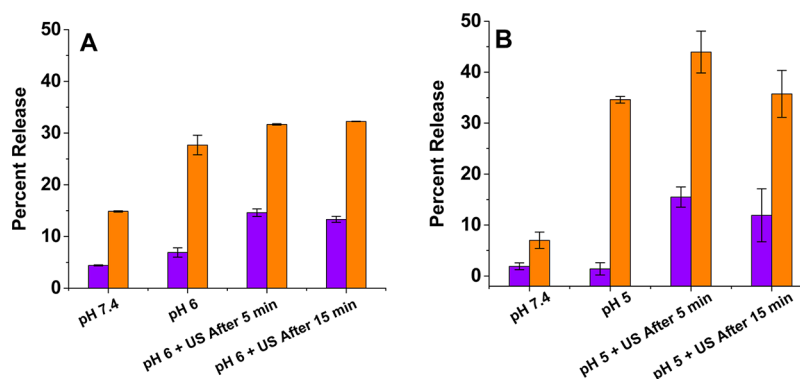


Figure 7. Ultrasound-enhanced (1 MHz, CW, 2 W/cm², 5 min), pH-triggered release from POPC liposomes encapsulating 200 of mM ammonium bicarbonate at pH = 6.0 (A) and pH = 5.0 (B). The release values at a pH of 7.4 are included as the controls. Violet bars: release after 20 min with ultrasound application. Orange bars: release after 2 h with ultrasound application ($n = 3$).

We employed tapping mode atomic force microscopic imaging to determine if the escaping gas bubbles caused any structural changes (shape and surface morphology) to the ammonium bicarbonate encapsulated POPC liposomes. After preparation, the ammonium bicarbonate encapsulated liposomes (pH = 7.4 buffer) were spherical with an average diameter around 100 nm (Figure 5A). However, after incubating in a pH 5.0 buffer for an hour, the liposomes fused, and the majority of the structures showed irregular shapes with sizes up to 800 nm (Figure 5B). These results demonstrated that the escaping gas bubbles caused permanent changes to the liposomes' morphology, leading to leakage of the encapsulated contents.

Triggered Release of Liposomal Contents with pH and Ultrasound. We reasoned that the released gas bubbles

inside the liposomes would allow an additional control on the contents released when employing high-frequency ultrasound. To test this hypothesis, we incubated the ammonium bicarbonate encapsulated (400 mM) POPC liposomes in buffers with pH of 6.0 (Figure 6A) and 5.0 (Figure 6B), and after 5 min, we exposed them to continuous wave ultrasound (1 MHz, 2 W/cm²) for 5 min. When incubated in a pH 5.0 buffer, 80% of the encapsulated contents were released from the liposomes in 2 h (compared to 55% released in the absence of ultrasound; Figure 6B). The corresponding content releases were considerably lower in pH 6.0 buffer (Figure 6A). Decreasing the concentration of encapsulated ammonium bicarbonate (from 400 mM to 200 mM) reduced the amount of contents released upon the application of ultrasound, to 45% (Figure 7). We also observed that the applied ultrasound

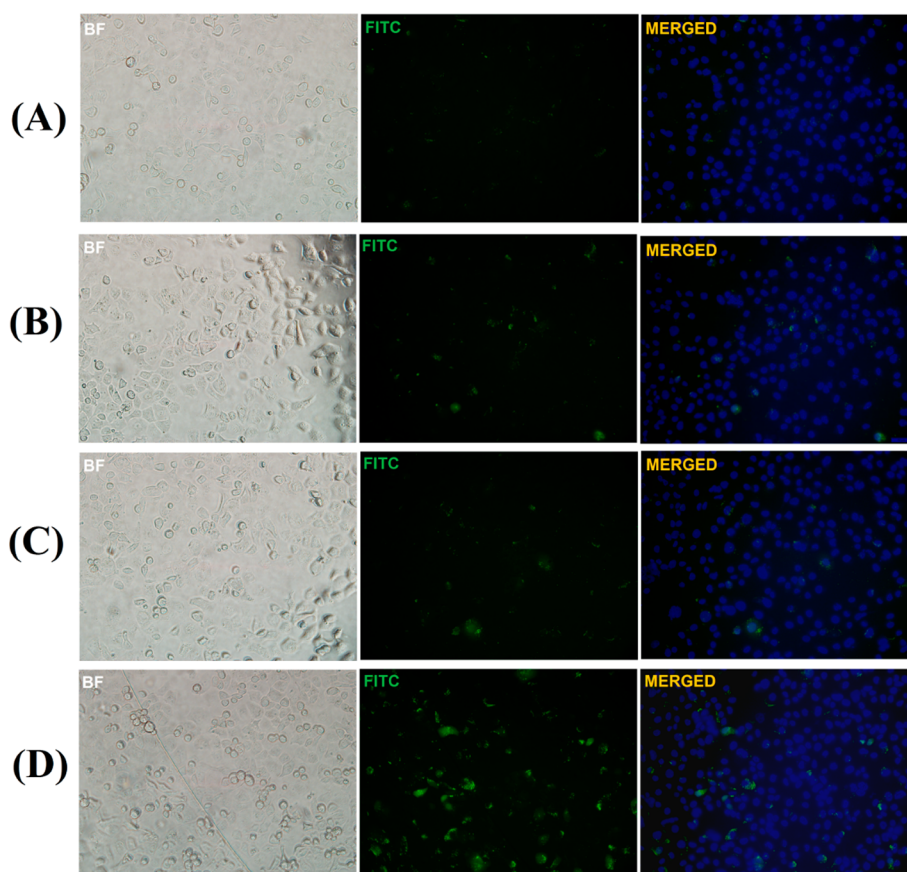


Figure 8. Fluorescence microscopic images for the uptake of pH-tunable, echogenic POPC liposomes encapsulating carboxyfluorescein by the folate receptor overexpressing PANC-1 cancer cells. Images were obtained using different filters: Brightfield (BF), fluorescein isothiocyanate (FITC, green fluorescence), and 4',6-diamino-2-phenylindole (DAPI, blue fluorescence). The images obtained with DAPI filter are not shown. DAPI and FITC images were merged using the ImageJ software and are shown. (A) Nontargeted liposomes after 3 h of incubation (magnification: 20 \times). (B) Nontargeted liposomes after 6 h of incubation (magnification: 20 \times). (C) Folate-targeted liposomes after 3 h of incubation (magnification: 20 \times). (D) Folate-targeted liposomes after 6 h of incubation (magnification: 20 \times).

exerted a maximum effect when applied within 5–15 min of incubating the liposomes with the pH 5 buffer. It is likely that the generated CO₂ bubbles escape from the liposomes within 15 min, and after that time, liposomes become less responsive to ultrasound. During the imaging studies, we observed a decrease in the echogenicity of the liposomes after 15 min of incubation in the pH 5 buffer (Figure 2).

When the ammonium bicarbonate encapsulated POPC liposomes were incubated in pH 6 buffer, we observed that applying the ultrasound enhanced the release by 15–20%. Contrary to the pH 5 experimental results, this enhancement in contents release was not strongly dependent on the time when the ultrasound was applied (Figures 6A and 7A). At a pH of 6, the concentration of hydronium ions was 10 times less compared to that at a pH of 5. The lower hydronium ion concentration at a pH of 5 contributed to a slow generation of gas bubbles inside the liposomes, and it took longer to consume the encapsulated ammonium bicarbonate. These two factors likely contributed to the results observed with ultrasound at a pH of 6.0.

We observed that applying ultrasound increased liposome solutions' temperature from 25 to 30 °C. It is possible that a thermal effect along with the mechanical effect could be responsible for the content release. To determine if this temperature change influenced the contents released from liposomes, we repeated the studies (in a pH 5 buffer) in a large

ice bath. The ice bath's temperature was maintained below 10 °C throughout the experiments. The results from these two experiments were identical, indicating that the temperature increase did not influence the contents released from our pH-sensitive liposomes.⁴² However, we note that one cannot rule out the possibility of local hot spots being generated in the liposomes themselves even when they are in the ice bath. Such temperature hotspot can only be created by the mechanical compression of the air cavity entrapped in the liposomes.⁴³

Internalization Studies with Pancreatic Cancer Cells.

Having optimized the ultrasound-enhanced release from the pH-sensitive liposomes, we proceeded to demonstrate the effectiveness of the strategy in cellular studies. To demonstrate efficient cellular internalization, we prepared liposomes incorporating 1 mol % 1,2-distearoyl-*sn*-glycero-3-phosphoethanolamine-*N*-[folate(polyethylene glycol)-5000] (ammonium salt, commercially available from Avanti Polar Lipids) and POPC encapsulating 100 mM carboxyfluorescein. We selected the folate receptor overexpressing pancreatic ductal carcinoma cells (PANC-1) for our cellular studies.⁴⁴

After incubating with the liposomes, we imaged the cells by employing a confocal fluorescence microscope. We noticed that liposomes incorporating 1 mol % of the folate lipid were taken up more effectively by the PANC-1 cells compared to the liposomes without the folate lipid (Figure 8). If the cells had a higher expression of the folate receptor, the internalization rate

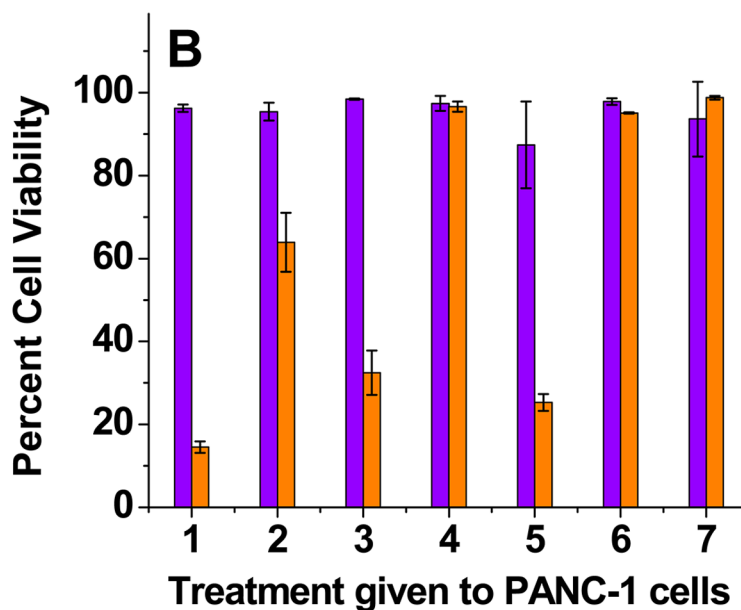
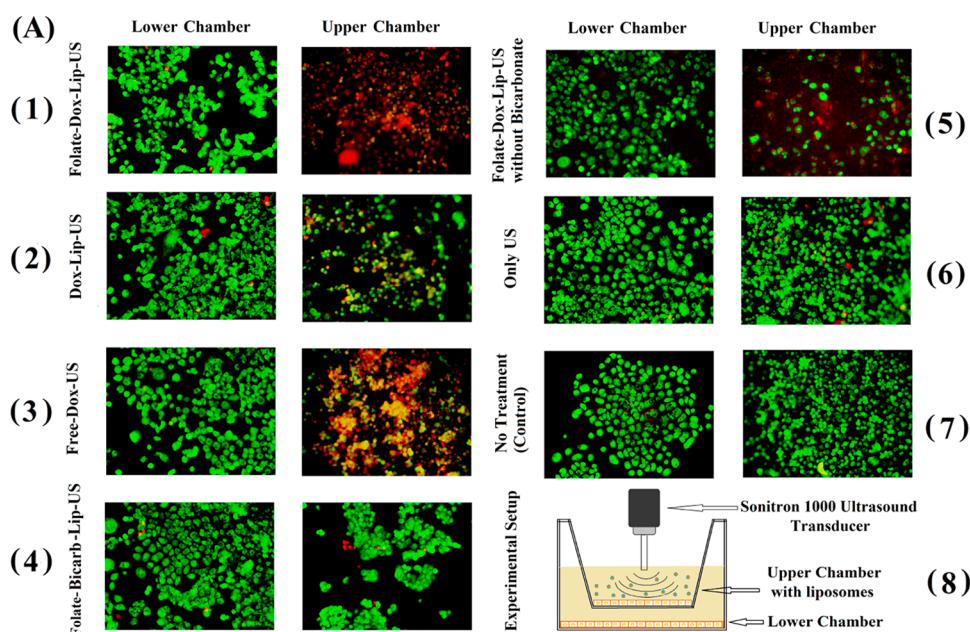


Figure 9. (A) PANC-1 cell viability studies using live (green) and dead (red) cell staining of different treatment groups ($n = 3$). The upper chamber cells received direct exposure, whereas the lower chamber cells received indirect exposure to POPC liposomes and ultrasound. (1) Folate-targeted doxorubicin liposomes (encapsulating ammonium bicarbonate) + ultrasound. (2) Nontargeted doxorubicin liposomes (encapsulating ammonium bicarbonate) + ultrasound. (3) Free doxorubicin + ultrasound. (4) Folate-targeted liposomes (encapsulating ammonium bicarbonate but no doxorubicin) + ultrasound. (5) Folate-targeted doxorubicin liposomes (no ammonium bicarbonate encapsulation) + ultrasound. (6) Ultrasound only. (7) No treatment (control). (8) Schematic representation of the experimental setup. The final doxorubicin concentration used was $25 \mu\text{g/mL}$. (B) Cell viability of the upper chamber (orange bars) and lower chamber (violet bars).

was faster. For example, the breast cancer cell line MCF-7 internalized the folate lipid containing liposomes faster compared to the PANC-1 cells (Supporting Information, Figure S6).

Intracellular Release of Liposomal Contents in Response to Reduced pH and the Application of Ultrasound. After confirming cellular internalization, we encapsulated the anticancer drug doxorubicin in the POPC liposomes and studied its release in the cytosol of the PANC-1 cells (in the absence and presence of applied diagnostic frequency ultrasound). Although gemcitabine is the standard

chemotherapeutic drug for pancreatic cancer, doxorubicin is currently being tested as a possible adjuvant therapy.^{45–47} We noted, *a priori*, that some literature reports question the safety of ultrasound for healthy tissues surrounding a tumor.⁴⁸ To determine if the ultrasound has any deleterious effects for the normal cells, we seeded the PANC-1 cells onto Transwell inserts consisting of two chambers. Diagnostic frequency ultrasound is reported to pass through the insert and reach the lower chamber.^{49,50} In this experimental design, the PANC-1 cells in the upper chamber represented the tumor tissue, receiving direct exposure to the liposomes as well as the applied

ultrasound. The cells in the lower chamber represented the neighboring tissue, which may be indirectly exposed to the treatment (Figure 9A). The pore size for the Transwell insert was 400 nm, and the average diameter for the liposomes was 110 nm. Hence, we expected that some liposomes and ultrasound waves would pass through the membrane to reach the lower chamber.^{49,50}

Upon reaching confluency, we exposed the upper chamber's cells to various combinations of targeted/nontargeted doxorubicin-encapsulated liposomes and ultrasound (applied between 15 and 20 min of incubation; Figure 9A). Subsequently, we placed the cells in an incubator for 6 h and stained to visualize the live and dead cells. We observed that indirect exposure to any of the treatments did not cause cell death in the lower chamber (Figures 9A and 9B). On the other hand, direct exposure to folate-targeted or nontargeted, pH-tunable, doxorubicin-encapsulated liposomes and ultrasound led to significant cell death in the upper chamber (Figures 9A and 9B).

We observed that the folate-targeted, doxorubicin and ammonium bicarbonate encapsulated POPC liposomes (Figure 9A-1) were more toxic (14% cell viability) compared to the corresponding liposomes without bicarbonate encapsulation (cell viability 25%; Figure 9A-5). It was reported that the cavitation force of exploding CO₂ bubbles in the lysosomes mechanically disrupts the membranes, leading to the release of lysosomal proteolytic enzymes in the cytosol and to cell death.^{34,42} Contrary to this report, we observed less than 5% cell death in the presence of liposomes that only encapsulate ammonium bicarbonate (i.e., without doxorubicin; Figure 9A-4). These results indicated that, in our experiments, cavitation induced by CO₂ bubbles enhanced the toxicity of the liposomal formulations.

Clearly, the folate-targeted doxorubicin liposomes (encapsulating ammonium bicarbonate) in the presence of applied ultrasound were most effective in killing the PANC-1 cells (Figures 9A-1 and 9B, group 1). This combination reduced the cell viability to 14% (Figure 9B, group 1). Interestingly, the free doxorubicin in the presence of applied ultrasound was more effective compared to liposomal doxorubicin (without folate) in inducing cell death (Figures 9A-2 and 9A-3). It is likely that sonoporation by the ultrasound is contributing to this effect. In the absence of any microbubbles, the pores formed in the cell membranes by the applied ultrasound are likely to be small and transient. Possibly, the sizes of these transient pores are large enough to allow doxorubicin molecules to cross the cell membranes.⁵¹ These observations are consistent with literature reports demonstrating a higher uptake of smaller particles compared to larger ones upon sonoporation.⁵² We observed that, under our experimental conditions, direct or indirect exposure to the ultrasound does not induce cell death (Figure 9A-6).

Our objective was not to compare the efficacy of free doxorubicin in the absence and presence of applied diagnostic-frequency ultrasound. Our goal was to determine the effectiveness of the ammonium bicarbonate and doxorubicin coencapsulated liposomes when ultrasound is applied. Numerous literature reports demonstrate the efficacy of doxorubicin for PANC-1 cells (without the applied ultrasound),^{53–55} hence, we did not include this control experiment.

PANC-1 is a metastatic pancreatic cancer cell line known to secrete matrix metalloproteinase (MMP) -2 and -9 enzymes in the extracellular matrix.⁵⁶ These two proteolytic enzymes are

responsible for the hydrolysis of the extracellular matrix, leading to the migration and metastasis of cancer cells.⁵⁷ Ultrasound treatment can loosen the extracellular material surrounding a tumor, resulting in the dissemination of cancer cells into the bloodstream. This action leads to increased migration and metastasis of the cancer cells when exposed to ultrasound.⁵⁸ To determine if our experimental conditions contribute to such effects, we conducted migration assays of the PANC-1 cells in the presence of applied ultrasound. For this endeavor, we seeded the PANC-1 cells onto an 8 μ m Transwell insert. After 6 h, we exposed the cells to ultrasound (1 MHz, 5 min), incubated them overnight, and determined their migration. We observed that there was no significant difference ($P > 0.01$, $n = 5$) in the migration ability of the ultrasound-exposed cells compared to the control samples (no ultrasound exposure). These results suggested that, within our experimental parameters, the migration of the PANC-1 cells remained unaffected by the applied ultrasound. Further *in vivo* validation studies with the ammonium bicarbonate encapsulated liposomes are in progress, and the results will be reported in the future.

CONCLUSIONS

We have successfully demonstrated the proof-of-concept for a new strategy to release liposomal contents in response to reduced pH. With our design, the liposomes encapsulate the gas precursor, ammonium bicarbonate, and do not incorporate pH-sensitive lipids in the bilayer. When incubated in buffers of acidic pH, CO₂ gas bubbles are generated, thus, inducing echogenicity to the liposomes. The escaping gas bubbles cause structural changes to the liposomes, and release the encapsulated contents (up to 56%). The content release is further enhanced by the simultaneous application of diagnostic-frequency ultrasound (1 MHz, 5 min; 80% release). The fluidity of the liposomal membranes plays a crucial role in the contents released. By incorporating a folate lipid in the bilayer, we have successfully targeted the liposomes to pancreatic cancer cells that overexpress the folate receptor on the surface. Liposome-encapsulated doxorubicin is efficiently released in the cancer cells, and the release is enhanced by the simultaneous application of diagnostic frequency ultrasound. While the ultrasound was innocuous, the combination of doxorubicin released from the liposomes and ultrasound reduced the viability of pancreatic cancer cells to 14%. With further developments, these liposomes have the potential to be an excellent option for ultrasound image guided, targeted drug delivery at tumor sites.

ASSOCIATED CONTENT

Supporting Information

Detailed experimental procedures for liposome preparation, release studies, cell culture, cellular release studies, fluorescence correction for carboxyfluorescein, pH-triggered release profiles of sodium bicarbonate encapsulated POPC liposomes, pH-triggered release from ammonium bicarbonate DSPC liposomes, and liposomal uptake studies with MCF-7 cells. This material is available free of charge via the Internet at <http://pubs.acs.org>.

■ AUTHOR INFORMATION

Corresponding Author

*Department of Pharmaceutical Sciences, North Dakota State University, Fargo, ND 58108-6050. E-mail: sanku.mallik@ndsu.edu. Tel: 701-231-7888. Fax: 701-231-8333.

Notes

The authors declare no competing financial interest.

■ ACKNOWLEDGMENTS

This research was supported by NIH Grant 1R01 CA 132034 to S.M. and D.K.S., NSF Grants DMR 1005011 and DMR 1306154 to S.M., and NSF Grant DMR 1005283 and NIH Grant P20RR016472 to K.S. We thank Dr. Jagdish Singh, Chair, Department of Pharmaceutical Sciences, for providing the Sonitron-1000 instrument for the ultrasound experiments.

■ REFERENCES

- (1) Kaye, S. B.; Richardson, V. J. Potential of liposomes as drug-carriers in cancer chemotherapy: a review. *Cancer Chemother. Pharmacol.* **1979**, *3* (2), 81–5.
- (2) Yang, F.; Jin, C.; Jiang, Y.; Li, J.; Di, Y.; Ni, Q.; Fu, D. Liposome based delivery systems in pancreatic cancer treatment: from bench to bedside. *Cancer Treat. Rev.* **2011**, *37* (8), 633–42.
- (3) Yu, X.; Zhang, Y.; Chen, C.; Yao, Q.; Li, M. Targeted drug delivery in pancreatic cancer. *Biochim. Biophys. Acta* **2010**, *1805* (1), 97–104.
- (4) Torchilin, V. P. Recent advances with liposomes as pharmaceutical carriers. *Nat. Rev. Drug Discovery* **2005**, *4* (2), 145–60.
- (5) Andresen, T. L.; Thompson, D. H.; Kaasgaard, T. Enzyme-triggered nanomedicine: drug release strategies in cancer therapy. *Mol. Membr. Biol.* **2010**, *27* (7), 353–63.
- (6) Elegbede, A. I.; Banerjee, J.; Hanson, A. J.; Tobwala, S.; Ganguli, B.; Wang, R.; Lu, X.; Srivastava, D. K.; Mallik, S. Mechanistic studies of the triggered release of liposomal contents by matrix metalloproteinase-9. *J. Am. Chem. Soc.* **2008**, *130* (32), 10633–42.
- (7) Sarkar, N. R.; Rosendahl, T.; Krueger, A. B.; Banerjee, A. L.; Benton, K.; Mallik, S.; Srivastava, D. K. “Uncorking” of liposomes by matrix metalloproteinase-9. *Chem. Commun. (Cambridge, U.K.)* **2005**, *8*, 999–1001.
- (8) Kulkarni, P. S.; Haldar, M. K.; Nahire, R. R.; Katti, P.; Ambre, A. H.; Muhonen, W. W.; Shabb, J. B.; Padi, S. K.; Singh, R. K.; Borowicz, P. P.; Shrivastava, D. K.; Katti, K. S.; Reindl, K.; Guo, B.; Mallik, S. MMP-9 Responsive PEG Cleavable Nanovesicles for Efficient Delivery of Chemotherapeutics to Pancreatic Cancer. *Mol. Pharmaceutics* **2014**, *11* (7), 2390–9.
- (9) Felber, A. E.; Dufresne, M. H.; Leroux, J. C. pH-sensitive vesicles, polymeric micelles, and nanospheres prepared with polycarboxylates. *Adv. Drug Delivery Rev.* **2012**, *64* (11), 979–92.
- (10) Leite, E. A.; Souza, C. M.; Carvalho-Junior, A. D.; Coelho, L. G.; Lana, A. M.; Cassali, G. D.; Oliveira, M. C. Encapsulation of cisplatin in long-circulating and pH-sensitive liposomes improves its antitumor effect and reduces acute toxicity. *Int. J. Nanomed.* **2012**, *7*, 5259–69.
- (11) Kim, H. K.; Van den Bossche, J.; Hyun, S. H.; Thompson, D. H. Acid-triggered release via dePEGylation of fusogenic liposomes mediated by heterobifunctional phenyl-substituted vinyl ethers with tunable pH-sensitivity. *Bioconjugate Chem.* **2012**, *23* (10), 2071–7.
- (12) Yao, L.; Daniels, J.; Wijesinghe, D.; Andreev, O. A.; Reshetnyak, Y. K. pH-LIP(R)-mediated delivery of PEGylated liposomes to cancer cells. *J. Controlled Release* **2013**, *167* (3), 228–37.
- (13) Wehunt, M. P.; Winschel, C. A.; Khan, A. K.; Guo, T. L.; Abdrakhmanova, G. R.; Sidorov, V. Controlled drug-release system based on pH-sensitive chloride-triggerable liposomes. *J. Liposome Res.* **2013**, *23* (1), 37–46.
- (14) Unnikrishnan, S.; Klivanov, A. L. Microbubbles as ultrasound contrast agents for molecular imaging: preparation and application. *Am. J. Roentgenol.* **2012**, *199* (2), 292–9.
- (15) Jing, Y.; Zhu, Y.; Yang, X.; Shen, J.; Li, C. Ultrasound-triggered smart drug release from multifunctional core-shell capsules one-step fabricated by coaxial electrospray method. *Langmuir* **2011**, *27* (3), 1175–80.
- (16) Wu, D.; Wan, M. A novel fluoride anion modified gelatin nanogel system for ultrasound-triggered drug release. *J. Pharm. Pharm. Sci.* **2008**, *11* (4), 32–45.
- (17) Huang, S. L.; MacDonald, R. C. Acoustically active liposomes for drug encapsulation and ultrasound-triggered release. *Biochim. Biophys. Acta* **2004**, *1665* (1–2), 134–41.
- (18) De Geest, B. G.; Skirtach, A. G.; Mamedov, A. A.; Antipov, A. A.; Kotov, N. A.; De Smedt, S. C.; Sukhorukov, G. B. Ultrasound-triggered release from multilayered capsules. *Small* **2007**, *3* (5), 804–8.
- (19) Figueiredo, M.; Esenaliev, R. PLGA Nanoparticles for Ultrasound-Mediated Gene Delivery to Solid Tumors. *J. Drug Delivery* **2012**, *2012*, 767839.
- (20) Zhang, H.; Jiang, H.; Wang, H.; Zhao, J.; Chen, B.; Wang, X. Ultrasound mediated drug-loaded nanoparticles crossing cell membranes as a new strategy to reverse cancer multidrug resistance. *J. Nanosci. Nanotechnol.* **2011**, *11* (3), 1834–40.
- (21) Nahire, R.; Haldar, M. K.; Paul, S.; Ambre, A. H.; Meghanni, V.; Layek, B.; Katti, K. S.; Gange, K. N.; Singh, J.; Sarkar, K.; Mallik, S. Multifunctional polymersomes for cytosolic delivery of gemcitabine and doxorubicin to cancer cells. *Biomaterials* **2014**, *35* (24), 6482–97.
- (22) Barati, A. H.; Mokhtari-Dizaji, M.; Mozdarani, H.; Bathaie, S. Z.; Hassan, Z. M. Treatment of murine tumors using dual-frequency ultrasound in an experimental in vivo model. *Ultrasound Med. Biol.* **2009**, *35* (5), 756–63.
- (23) Shaw, G. J.; Meunier, J. M.; Huang, S. L.; Lindsell, C. J.; McPherson, D. D.; Holland, C. K. Ultrasound-enhanced thrombolysis with tPA-loaded echogenic liposomes. *Thromb. Res.* **2009**, *124* (3), 306–10.
- (24) Schroeder, A.; Honen, R.; Turjeman, K.; Gabizon, A.; Kost, J.; Barenholz, Y. Ultrasound triggered release of cisplatin from liposomes in murine tumors. *J. Controlled Release* **2009**, *137* (1), 63–8.
- (25) Ahmadi, F.; McLoughlin, I. V.; Chauhan, S.; ter-Haar, G. Bio-effects and safety of low-intensity, low-frequency ultrasonic exposure. *Prog. Biophys. Mol. Biol.* **2012**, *108* (3), 119–38.
- (26) Alkan-Onyuksel, H.; Demos, S. M.; Lanza, G. M.; Vonesh, M. J.; Klegerman, M. E.; Kane, B. J.; Kuszak, J.; McPherson, D. D. Development of inherently echogenic liposomes as an ultrasonic contrast agent. *J. Pharm. Pharm. Sci.* **1996**, *85* (5), 486–90.
- (27) Paul, S.; Nahire, R.; Mallik, S.; Sarkar, K. Encapsulated microbubbles and echogenic liposomes for contrast ultrasound imaging and targeted drug delivery. *Comput. Mech.* **2014**, *53* (3), 413–35.
- (28) Nahire, R.; Haldar, M. K.; Paul, S.; Mergoum, A.; Ambre, A. H.; Katti, K. S.; Gange, K. N.; Srivastava, D. K.; Sarkar, K.; Mallik, S. Polymer-coated echogenic lipid nanoparticles with dual release triggers. *Biomacromolecules* **2013**, *14* (3), 841–53.
- (29) Radhakrishnan, K.; Haworth, K. J.; Huang, S. L.; Klegerman, M. E.; McPherson, D. D.; Holland, C. K. Stability of echogenic liposomes as a blood pool ultrasound contrast agent in a physiologic flow phantom. *Ultrasound Med. Biol.* **2012**, *38* (11), 1970–81.
- (30) Kopechek, J. A.; Haworth, K. J.; Raymond, J. L.; Douglas Mast, T.; Perrin, S. R.; Klegerman, M. E.; Huang, S.; Porter, T. M.; McPherson, D. D.; Holland, C. K. Acoustic characterization of echogenic liposomes: frequency-dependent attenuation and backscatter. *J. Acoust. Soc. Am.* **2011**, *130* (5), 3472–81.
- (31) Paul, S.; Russakow, D.; Nahire, R.; Nandy, T.; Ambre, A. H.; Katti, K.; Mallik, S.; Sarkar, K. In vitro measurement of attenuation and nonlinear scattering from echogenic liposomes. *Ultrasonics* **2012**, *52* (7), 962–969.
- (32) Smith, D. A.; Porter, T. M.; Martinez, J.; Huang, S.; MacDonald, R. C.; McPherson, D. D.; Holland, C. K. Destruction thresholds of echogenic liposomes with clinical diagnostic ultrasound. *Ultrasound Med. Biol.* **2007**, *33* (5), 797–809.

- (33) Nahire, R.; Paul, S.; Scott, M. D.; Singh, R. K.; Muhonen, W. W.; Shabb, J.; Gange, K. N.; Srivastava, D. K.; Sarkar, K.; Mallik, S. Ultrasound enhanced matrix metalloproteinase-9 triggered release of contents from echogenic liposomes. *Mol. Pharmaceutics* **2012**, *9* (9), 2554–64.
- (34) Chen, K. J.; Liang, H. F.; Chen, H. L.; Wang, Y.; Cheng, P. Y.; Liu, H. L.; Xia, Y.; Sung, H. W. A thermoresponsive bubble-generating liposomal system for triggering localized extracellular drug delivery. *ACS Nano* **2013**, *7* (1), 438–46.
- (35) Stathis, A.; Moore, M. J. Advanced pancreatic carcinoma: current treatment and future challenges. *Nat. Rev. Clin. Oncol.* **2010**, *7* (3), 163–172.
- (36) Klein, A. P. Identifying people at a high risk of developing pancreatic cancer. *Nat. Rev. Cancer* **2013**, *13* (1), 66–74.
- (37) Kremkau, F. W. *Diagnostic Ultrasound; Principles and Instrumentations*; Saunders: Philadelphia, 2002.
- (38) Kopechek, J. A.; Haworth, K. J.; Radhakrishnan, K.; Huang, S. L.; Klegerman, M. E.; McPherson, D. D.; Holland, C. K. The impact of bubbles on measurement of drug release from echogenic liposomes. *Ultrasonics Sonochem.* **2013**, *20* (4), 1121–30.
- (39) Davis, P. J.; Fleming, B. D.; Coolbear, K. P.; Keough, K. M. Gel to liquid-crystalline transition temperatures of water dispersions of two pairs of positional isomers of unsaturated mixed-acid phosphatidylcholines. *Biochemistry* **1981**, *20* (12), 3633–6.
- (40) Chen, R. F.; Knutson, J. R. Mechanism of fluorescence concentration quenching of carboxyfluorescein in liposomes: energy transfer to nonfluorescent dimers. *Anal. Biochem.* **1988**, *172* (1), 61–77.
- (41) Shimshick, E. J.; McConnell, H. M. Lateral phase separation in phospholipid membranes. *Biochemistry* **1973**, *12* (12), 2351–60.
- (42) Chung, M. F.; Chen, K. J.; Liang, H. F.; Liao, Z. X.; Chia, W. T.; Xia, Y.; Sung, H. W. A liposomal system capable of generating CO₂ bubbles to induce transient cavitation, lysosomal rupturing, and cell necrosis. *Angew. Chem., Int. Ed.* **2012**, *51* (40), 10089–93.
- (43) Leighton, T. G. *The acoustic bubble*, first printing pbk. ed.; Academic Press: San Diego, London, 1997; p xxvi, 613 pp.
- (44) Liang, M.; Lu, J.; Kovoichich, M.; Xia, T.; Ruehm, S. G.; Nel, A. E.; Tamanoi, F.; Zink, J. I. Multifunctional Inorganic Nanoparticles for Imaging, Targeting, and Drug Delivery. *ACS Nano* **2008**, *2* (5), 889–96.
- (45) Kratz, F.; Azab, S.; Zeisig, R.; Fichtner, I.; Warnecke, A. Evaluation of combination therapy schedules of doxorubicin and an acid-sensitive albumin-binding prodrug of doxorubicin in the MIA PaCa-2 pancreatic xenograft model. *Int. J. Pharm.* **2013**, *441* (1–2), 499–506.
- (46) Syrigos, K. N.; Michalaki, B.; Alevyzaki, F.; Machairas, A.; Mandrekas, D.; Kindilidis, K.; Karatzas, G. A phase-II study of liposomal doxorubicin and docetaxel in patients with advanced pancreatic cancer. *Anticancer Res.* **2002**, *22* (6B), 3583–8.
- (47) Halford, S.; Yip, D.; Karapetis, C. S.; Strickland, A. H.; Steger, A.; Khawaja, H. T.; Harper, P. G. A phase II study evaluating the tolerability and efficacy of CAELYX (liposomal doxorubicin, Doxil) in the treatment of unresectable pancreatic carcinoma. *Ann. Oncol.* **2001**, *12* (10), 1399–402.
- (48) Mitragotri, S. Healing sound: the use of ultrasound in drug delivery and other therapeutic applications. *Nat. Rev. Drug Discovery* **2005**, *4* (3), 255–60.
- (49) Cochran, M. C.; Eisenbrey, J.; Ouma, R. O.; Soulen, M.; Wheatley, M. A. Doxorubicin and paclitaxel loaded microbubbles for ultrasound triggered drug delivery. *Int. J. Pharm.* **2011**, *414* (1–2), 161–70.
- (50) Huang, S. L.; McPherson, D. D.; Macdonald, R. C. A method to co-encapsulate gas and drugs in liposomes for ultrasound-controlled drug delivery. *Ultrasound Med. Biol.* **2008**, *34* (8), 1272–80.
- (51) Lentacker, I.; Geers, B.; Demeester, J.; De Smedt, S. C.; Sanders, N. N. Design and evaluation of doxorubicin-containing microbubbles for ultrasound-triggered doxorubicin delivery: cytotoxicity and mechanisms involved. *Mol. Ther.* **2010**, *18* (1), 101–8.
- (52) Mehier-Humbert, S.; Bettinger, T.; Yan, F.; Guy, R. H. Plasma membrane poration induced by ultrasound exposure: implication for drug delivery. *J. Controlled Release* **2005**, *104* (1), 213–22.
- (53) Zirvi, K. A.; Hill, G. J. Comparison of growth and drug response of human tumor cells in serum-free and serum-supplemented media in human tumor-clonogenic assay. *J. Surg. Oncol.* **1988**, *38* (2), 88–93.
- (54) Wilkoff, L. J.; Dulmage, E. A. Sensitivity of proliferating cultured murine pancreatic tumor cells to selected antitumor agents. *J. Natl. Cancer Inst.* **1986**, *77* (5), 1163–9.
- (55) Chang, B. K. Comparison of in vitro methods for assessing cytotoxic activity against two pancreatic adenocarcinoma cell lines. *Cancer Res.* **1983**, *43* (7), 3147–9.
- (56) Takada, M.; Hirata, K.; Ajiki, T.; Suzuki, Y.; Kuroda, Y. Expression of receptor for advanced glycation end products (RAGE) and MMP-9 in human pancreatic cancer cells. *Hepato-Gastroenterology* **2004**, *51* (58), 928–30.
- (57) Ellenrieder, V.; Alber, B.; Lacher, U.; Hendler, S. F.; Menke, A.; Boeck, W.; Wagner, M.; Wilda, M.; Friess, H.; Buchler, M.; Adler, G.; Gress, T. M. Role of MT-MMPs and MMP-2 in pancreatic cancer progression. *Int. J. Cancer* **2000**, *85* (1), 14–20.
- (58) Frenkel, V. Ultrasound media-ated delivery of drugs and genes to solid tumors. *Adv. Drug Delivery Rev.* **2008**, *60* (10), 1193–208.